 doi:10.20944/preprints202011.0244.v1

Article

Uncertainty Assessment for Determining the Discharge Coefficient C for a Multi-Opening Orifice

Andrzej Mrowiec

The President Stanisław Wojciechowski Academy in Kalisz, Department of Technology; Poznańska 201-205, 62-800 Kalisz, Poland; a.mrowiec@akademiakaliska.edu.pl; Tel.: +48-606-942-976 (F.L.)

Abstract: The article contains the results of experimental studies for a multi-opening orifice with substitute constriction factor of $\beta = 0.5$ ($m = 0.25$), mounted in a DN50 hydraulic measuring flume. Flow measurements were taken for a progressing turbulent flow within Reynolds numbers (Re = 4700...19500). Based on experimental data, flow characteristics as well as discharge coefficient C characteristics were determined. Relative expanded uncertainty of determining a discharge coefficient C was estimated within the changes of volume flow q_v from 0.35 dm^3/s to 0.68 dm^3/s. The value does not exceed 1.25% within the changes of Reynolds numbers $9800 \leq Re \leq 19500$.

Keywords: volume flow; multi-opening orifice; experimental studies; measurement uncertainty analysis

1. Introduction

Fluid mechanics faces problems of measurement with volume flow on a micro-scale, which include, among others, biological systems, especially blood flow measurement [1], and on a macro-scale, in industrial flows. Several different flow meters are used for measuring, mainly for the purpose of controlling the technological process where constant measurement of fluid flow is required. The most common, as well as cheap and reliable devices to do the job, are wedge meters. They utilize sudden constriction of the pipeline which the fluid comes across. Fluid speed rapidly rises in the constriction, which results in a difference in static pressure before and behind the constricting segment. The following are normally used as flow bank-up constriction devices: Venturi tubes, nozzles, and measuring orifices [2 - 4]. Orifices are popular with measurement, despite their weaknesses, such as permanent loss of pressure with fluid flow and low rangeability (4:1). Among commonly known measuring orifices, the standard (centrical) orifice, characterized by accuracy at 1.5…2% was accepted as a basic model [5, 6]. A great number of researchers around the globe are searching for new solutions for metering orifices to measure fluid flow, which would be characterized by a constant value of discharge coefficient C in a wide range of changes in Reynolds numbers [7, 8]. Such a solution seems to come in the form of a flow meter with a flow choking element – a multi-opening orifice. It features more than one opening, usually cylindrical, in the orifice being the flow choking element. Subject literature normally presents results of numerical simulation studies of such orifices, with different number of holes and different position in the flow plane [9 – 11]. For this reason, there is often a lack of experimental studies and resulting attempts to estimate measurement uncertainty. With the traditional approach to calculating uncertainty, we use the rules from GUM international standard [12] where uncertainty is defined as a parameter of distribution of measurement error probability. With such an approach to the problem of uncertainty assessment, two types of standard uncertainties are determined: type A and type B [13]. To assess type A standard uncertainty, we use statistical analysis from a series of observations conducted in the same measuring conditions. It is estimated as the experimental standard deviation of mean resulting from averaging procedure and presents a measure of dispersion of measurement values around arithmetic mean [14]. Whereas, correct assessment of type B uncertainty results from familiarity with measuring

Preprints (www.preprints.org) | NOT PEER-REVIEWED | Posted: 6 November 2020 doi:10.20944/preprints202011.0244.v1

instruments used in the experiment. That is why it is most often estimated on the basis of accuracy of the measuring instruments used (information from the manufacturer or past familiarity with the instrument). A great deal of knowledge and experience of accepting or assuming the distribution of probability density function for the obtained measurement results is required from the experimenter when making the assessment. Whereby, expanded uncertainty is normally given as estimated measurement uncertainty, requiring the calculated type A and B uncertainties to be first geometrically put together, and then multiplied by coverage factor k_p [12].

The purpose of the conducted fluid flow studies described in the article is to analyze the metrological properties of the selected multi-opening orifice with substitute constriction factor of $\beta = 0.5$ ($m = 0.25$) and to determine a discharge coefficient C. Moreover, an attempt has been made to estimate the relative expanded uncertainty of determining the ratio in a progressing turbulent flow for Reynolds numbers from range $Re = 4700...19500$ in laboratory conditions.

2. The subject of study and measurement result

The study was conducted in laboratory conditions in Fluid Mechanics Laboratory in Department of Technology at The President Stanisław Wojciechowski Academy in Kalisz.

For experimental studies, a four-opening orifice was designed, taking into consideration all the recommendations used when designing a centrical orifice [5, 6]. An orifice designed this way was made of brass. Figure 1 presents the image and production drawing of the orifice.

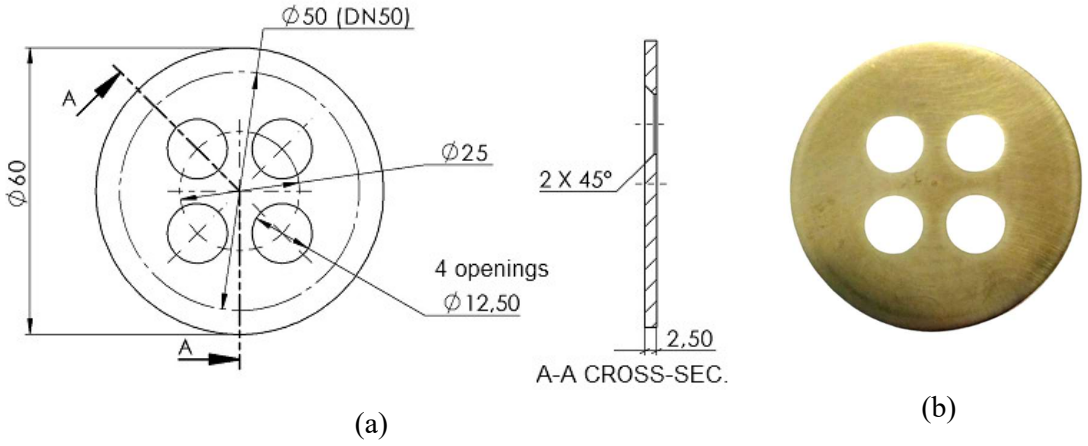

Figure 1. Multi-opening orifice model: (a) production drawing; (b) brass orifice.

It was placed in housing to allow the measurement of the bank-up pressure (the measurement of the difference in pressure before and behind the orifice) nearby. The orifice was mounted in the housing in a standard manner, where the inflow was directed at the sharp edges of flow openings, and the pressure measurement pulse openings were located on an axis between them.

The water testing station was built with two straight and smooth pipeline segments – DN50 and DN15, connected with a bend forming a 180° angle so that the pipelines would be parallel. The tested orifice (Fig. 1) was installed in the DN50 straight pipeline with total length 82·D. To shape the inlet speed profile, the straight segment before the orifice was 46·D (2.3 m) long, and 36·D (1.8 m) long behind the orifice. A magnetic flow meter was installed in the DN15 straight pipeline, according to the manual. It functions as the standard/model flow meter in the measuring system where straight segments were taken: 100·D before the flow meter and 50·D behind it. Figure 2 presents the diagram of the water hydraulic flow system.

Preprints (www.preprints.org) | NOT PEER-REVIEWED | Posted: 6 November 2020 doi:10.20944/preprints202011.0244.v1

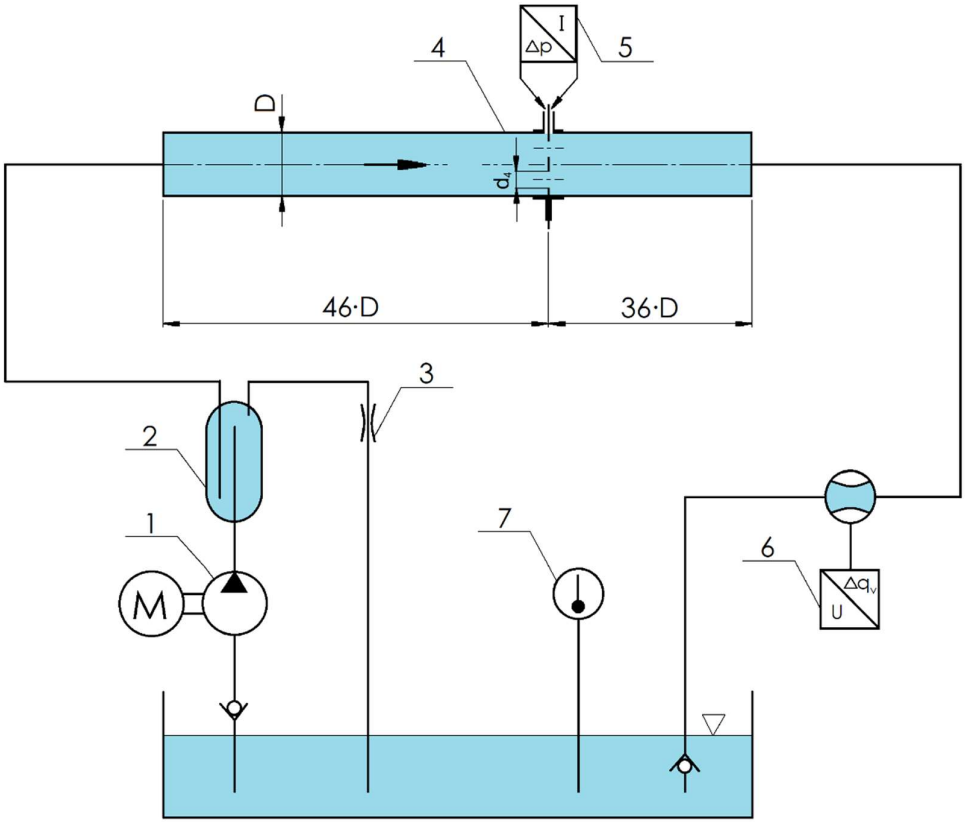

Figure 2. Block scheme of the hydraulic testing station.

The water stream produced by the centrifugal pump (1) flows through the vent (2). In the air vent system, any air bubbles are separated and removed from the fluid stream generated by the pump through the so-called side discharge. It is equipped with replaceable chokes (3), which allow for an additional step adjustment of the flowing water stream through the measuring system of the hydraulic pipeline (4).

The diameter of pipeline D and the flow-through openings d_4 in the orifice was measured with a slide caliper with digital display (with resolving power at 0,01 mm) for which limiting error is 0.05 mm. Pressure bank-up on the tested orifice was measured in close proximity with an APR-2000/ALW differential pressure transducer (5). It was programmed for pressure difference measuring range of $\Delta p = 0…2.4$ kPa with a measuring error of 0.15% and time-constant $t = 5$ s with output current signal 4…20 mA.

Water stream in the system also flows through the PROMAG 30AT15 magnetic flow meter (6) (used as standard/model in the measuring system). It was set for stream volume in measuring range $q_v = 0…1.0$ dm³/s with measuring error at $\Delta_{qv} = \pm(0.2\% \cdot q_{v\text{-}measured} \pm 0.05\% \cdot q_v)$ with time-constant $t = 5$ s and output current signal 0…20 mA.

In the presented measuring system, both the volume stream and water temperature were measured simultaneously for each measurement series, the latter measured with a thermometer (7). Flow parameters (signals from the flow meter and the differential pressure transducer) were recorded using SANWA 5000 multimeters connected to a computer measuring system on a PC, using RS-232 interface. The computer used specialized PC Link Plus software which allowed to acquire measurement data with a preset sampling time at $\Delta t = 6$ s. A total of 12 volume streams were tested on the described station, with streams q_v ranging 0.167…0.683 dm³/s (for Reynolds numbers ranging $Re = 4700...19500$). The measurements were taken for a stabilized stream of flowing water, recording 12 series of observations each, and each of the recorded series was averaged from 20 single measurements.

Preprints (www.preprints.org) | NOT PEER-REVIEWED | Posted: 6 November 2020 doi:10.20944/preprints202011.0244.v1

The acquisition of measurement data involved recording the following parameters: volume stream q_v, pressure difference on orifice Δp, and water temperature T. For all measurement series the water temperature did not exceed 1.5°C during the study. Table 1 presents the geometry of pipeline D, geometry of orifice flow-through openings d_4 and averaged results of experimental measurements (T, q_v, Δp) and corresponding values from calculations: the value of Reynolds numbers Re and discharge coefficient C.

Table 1. Results of experimental measurements.

D	d	T	q_v	Δp	Re	C
[mm]	[mm]	[°C]	[dm³/s]	[Pa]	[-]	[-]
50.20	12.54	25.30	0.6825	2289.4	19479	0.6283
50.26	12.53	25.40	0.6536	2098.9	18696	0.6284
50.37	12.53	25.40	0.6202	1891.1	17740	0.6282
50.28	12.52	25.35	0.5907	1715.4	16879	0.6283
50.31	12.52	25.25	0.5580	1533.0	15909	0.6278
50.36	12.51	25.20	0.5196	1327.5	14798	0.6283
50.26	12.51	25.10	0.4858	1160.2	13802	0.6283
50.25	12.52	25.00	0.4590	1035.0	13012	0.6285
50.40	12.51	24.95	0.4145	843.1	11739	0.6289
50.22	12.53	24.90	0.3456	581.9	9774	0.6310
50.35	12.52	24.85	0.2537	310.4	7168	0.6344
50.24	12.52	24.75	0.1666	130.0	4697	0.6439

Based on the results of experimental measurements (Table 1) a flow characteristics was made for the tested multi-opening orifice with module $m = 0.25$ (see Figure 3). The characteristics are described with a power equation with the coefficient of determination close to 1 which indicates a very good adjustment of the designated model (trend line) to the averaged results obtained from the experiment.

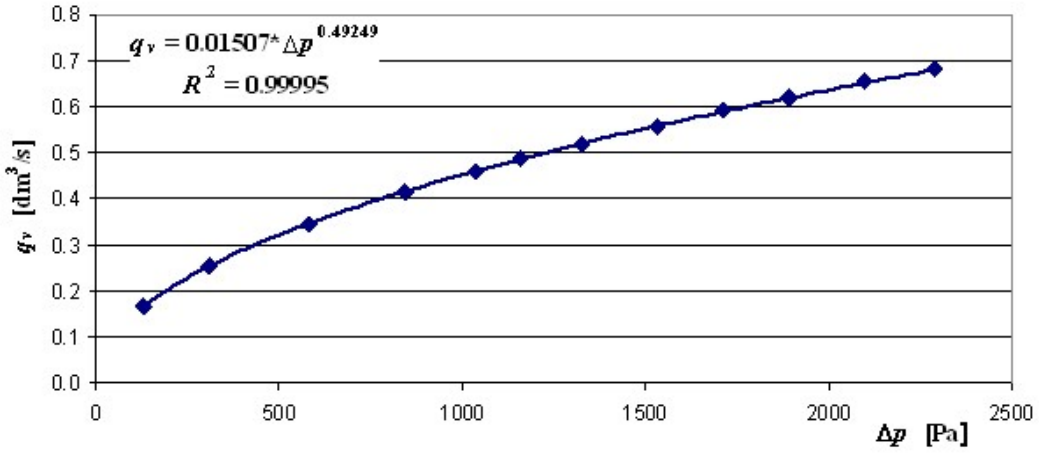

Figure 3. Flow characteristics of the tested orifice $q_v = f(\Delta p)$.

3. Determining the uncertainty of discharge coefficient

This chapter presents the results of the conducted analysis of determining the uncertainty [12, 13] of discharge coefficient C through the tested multi-opening orifice. Fluid volume stream q_v flowing through the tested multi-opening orifice can be described with a known dependence (1) [5] as:

 doi:10.20944/preprints202011.0244.v1

$$q_v = \frac{C \cdot \varepsilon \cdot F_{04}}{\sqrt{1-m^2}} \cdot \sqrt{\frac{2 \cdot \Delta p}{\rho}} \tag{1}$$

where: C - discharge coefficient,

ε - expansion factor

F_{04} - orifice constriction area [m²],

m - orifice module,

Δp - pressure difference before and behind the orifice in [Pa],

ρ - fluid density [kg/m³].

The orifice constriction cross-section area is composed of four identical openings with diameter d_4 (Fig. 1) and is presented with a dependence (2):

$$F_{04} = \frac{4 \cdot \pi \cdot d_4^2}{4} = \pi \cdot d_4^2 \tag{2}$$

It was assumed that the ratio of constriction cross-section area F_{04} to pipeline cross-section F_D is module m of the orifice. In further deliberations, an individual constriction of a single opening of the four-opening orifice was introduced as $\beta_4 = d_4/D$ (the following diameters were considered in flow cross-sections: diameter of pipeline D and d_4 as one of four identical openings in the multi-opening orifice). The result was a dependence (3):

$$m = \frac{F_{04}}{F_D} = \frac{4 \cdot d_4^2}{D^2} = 4 \cdot \beta_4^2 \tag{3}$$

Assuming incompressibility of flowing water (ε = 1) for experimental studies and considering dependence (2) and (3) in the formula (1), an expression for volume stream was obtained (4):

$$q_v = C \cdot \pi \cdot \frac{d_4^2}{\sqrt{1-16 \cdot \beta_4^4}} \cdot \sqrt{\frac{2 \cdot \Delta p}{\rho}} \tag{4}$$

By transforming the designated dependence (4) a formula for discharge coefficient C was determined in the following form (5):

$$C = \frac{q_v \cdot \sqrt{1-16 \cdot \beta_4^4}}{\pi \cdot d_4^2 \cdot \sqrt{\frac{2 \cdot \Delta p}{\rho}}} \tag{5}$$

For discharge coefficient defined in such way (5), the standard relative uncertainty of its determination $u(C)/C$ was calculated. It was determined from measurements of the measured values, indirectly according to the propagation of uncertainty rule [12] from formula (6):

$$\frac{u(C)}{C} = \left[\left(\frac{1}{C} \cdot \frac{\partial C}{\partial q_v} \cdot u(q_v) \right)^2 + \left(\frac{1}{C} \cdot \frac{\partial C}{\partial \Delta p} \cdot u(\Delta p) \right)^2 + \left(\frac{1}{C} \cdot \frac{\partial C}{\partial \rho} \cdot u(\rho) \right)^2 + \right. \tag{6}$$

Preprints (www.preprints.org) | NOT PEER-REVIEWED | Posted: 6 November 2020 doi:10.20944/preprints202011.0244.v1

$$+\left(\frac{1}{C}\cdot\frac{\partial C}{\partial d_4}\cdot u(d_4)\right)^2+\left(\frac{1}{C}\cdot\frac{\partial C}{\partial D}\cdot u(D)\right)^2\Bigg]^{0,5}$$

Next, based on dependence (6), partial derivatives were determined. When multiplied by converse discharge coefficient (5), they yield components of equation (6). They are presented in Table 2.

Table 2. Components determined from equation (6).

Partial derivatives	Equation (6) components	
$\frac{\partial C}{\partial q_v}=\frac{\sqrt{1-16\cdot\beta_4^4}}{\pi\cdot d_4^2\cdot\sqrt{\frac{2\cdot\Delta p}{\rho}}}$	$\frac{1}{C}\cdot\frac{\partial C}{\partial q_v}=\frac{1}{q_v}$	(7)
$\frac{\partial C}{\partial \Delta p}=\frac{q_v\cdot\sqrt{1-16\cdot\beta_4^4}}{\pi\cdot d_4^2\cdot\sqrt{\frac{2\cdot\Delta p}{\rho}}}\cdot\frac{(-1)}{2\cdot\Delta p}$	$\frac{1}{C}\cdot\frac{\partial C}{\partial \Delta p}=-\frac{1}{2}\cdot\frac{1}{\Delta p}$	(8)
$\frac{\partial C}{\partial \rho}=\frac{q_v\cdot\sqrt{1-16\cdot\beta_4^4}}{\pi\cdot d_4^2\cdot\sqrt{\frac{2\cdot\Delta p}{\rho}}}\cdot\frac{1}{2\cdot\rho}$	$\frac{1}{C}\cdot\frac{\partial C}{\partial \rho}=\frac{1}{2}\cdot\frac{1}{\rho}$	(9)
$\frac{\partial C}{\partial d_4}=\frac{q_v}{\pi\cdot\sqrt{\frac{2\cdot\Delta p}{\rho}}}\cdot\left(\frac{-2}{d_4^3\cdot\sqrt{1-16\cdot\beta_4^4}}\right)$	$\frac{1}{C}\cdot\frac{\partial C}{\partial d_4}=-\frac{2}{1-16\cdot\beta_4^4}\cdot\frac{1}{d_4}$	(10)
$\frac{\partial C}{\partial D}=\frac{q_v}{\pi\cdot\sqrt{\frac{2\cdot\Delta p}{\rho}}}\cdot\frac{32\cdot\beta_4^2}{D^3\cdot\sqrt{1-16\cdot\beta_4^4}}$	$\frac{1}{C}\cdot\frac{\partial C}{\partial D}=\frac{32\cdot\beta_4^4}{1-16\cdot\beta_4^4}\cdot\frac{1}{D}$	(11)

After substituting components of equations (7) to (11) in equation (6) for combined relative standard uncertainty of determining discharge coefficient $u(C)/C$, the dependence (12) was obtained:

$$\frac{u(C)}{C}=\Bigg[\left(\frac{u(q_v)}{q_v}\right)^2+\frac{1}{4}\cdot\left(\frac{u(\Delta p)}{\Delta p}\right)^2+\frac{1}{4}\cdot\left(\frac{u(\rho)}{\rho}\right)^2+\left(\frac{2}{1-16\cdot\beta_4^4}\right)^2\cdot\left(\frac{u(d_4)}{d_4}\right)^2+$$
$$+\left(\frac{32\cdot\beta_4^4}{1-16\cdot\beta_4^4}\right)^2\cdot\left(\frac{u(D)}{D}\right)^2\Bigg]^{0,5} \quad (12)$$

Table 3 presents relative standard components of uncertainty, present in equation (12), necessary for calculating the combined relative standard uncertainty of discharge coefficient $u(C)/C$.

Table 3. Relative standard components of the uncertainty of equation (12).

$\frac{u(q_v)}{q_v}=\frac{\sqrt{S_{(q_v)}^2+\left(\frac{\Delta_{(q_v)}}{\sqrt{3}}\right)^2}}{q_v}\cdot 100\%$	**(13)**

Preprints (www.preprints.org) | NOT PEER-REVIEWED | Posted: 6 November 2020 doi:10.20944/preprints202011.0244.v1

$$\frac{u(\Delta p)}{\Delta p} = \frac{\sqrt{S^2_{(\Delta p)} + \left(\frac{\Delta_{(\Delta p)}}{\sqrt{3}}\right)^2}}{\Delta p} \cdot 100\% \quad (14)$$

$$\frac{u(\rho)}{\rho} = \frac{\frac{\Delta_{(\rho)}}{\sqrt{3}}}{\rho} \cdot 100\% \quad (15)$$

$$\frac{u(d_4)}{d_4} = \frac{\sqrt{S^2_{(d_4)} + \left(\frac{\Delta_{(d_4)}}{\sqrt{3}}\right)^2}}{d_4} \cdot 100\% \quad (16)$$

$$\frac{u(D)}{D} = \frac{\sqrt{S^2_{(D)} + \left(\frac{\Delta_{(D)}}{\sqrt{3}}\right)^2}}{D} \cdot 100\% \quad (17)$$

Experimental standard deviations S that exist in formulas (13)…(17) represent type A random uncertainties of average measured values. With 12 observations conducted, the deviations were increased by Student's distribution critical factor ($k_n = 2.2$) with assumed confidence level $p = 0.95$. In order to determine type B uncertainty, a rectangular distribution of probability was assumed, where the Δ symbol marked absolute maximum limiting errors of input value data measurements, resulting from the use of the measuring instruments. Eventually, following the EN ISO 5167-1 standard [5] and dependence (12), we can determine the relative expanded uncertainty of discharge coefficient $U(C)/C$ (for confidence level p = 95% with coverage factor $k_p = 2$) for the multi-opening orifice and write it down in the form of formula (18):

$$\frac{U(C)}{C} = k_p \cdot \frac{u(C)}{C} \quad (18)$$

Figure 4 presents values of relative expanded uncertainty of discharge coefficient $U(C)/C$, based on experimental studies, in a form of dots, for the multi-opening orifice (Fig. 1) within the range of volume stream change $q_v = 0.167…0.683$ dm³/s.

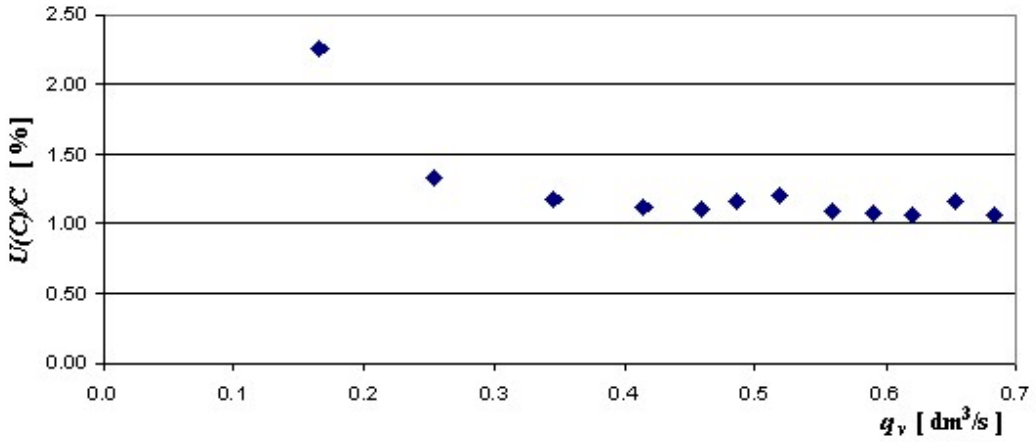

Figure 4. Distribution of relative expanded uncertainty of flow ratio $U(C)/C$ dependent upon volume stream q_v.

When analyzing the presented graph, we may state that the relative expanded uncertainty of determining discharge coefficient $U(C)/C$ does not exceed 1.25% for volume stream $q_v \geq 0{,}35$ dm³/s in

Preprints (www.preprints.org) | NOT PEER-REVIEWED | Posted: 6 November 2020 doi:10.20944/preprints202011.0244.v1

the studied measurement range. On the other hand, Figure 5 presents values of discharge coefficient *C*, determined on the basis of the conducted experimental studies, in the function of Reynolds numbers (*Re* = 4700...19500) with bars representing errors that result from calculating its expanded uncertainty *U(C)* with coverage factor $k_p = 2$ and confidence level $p = 0.95$.

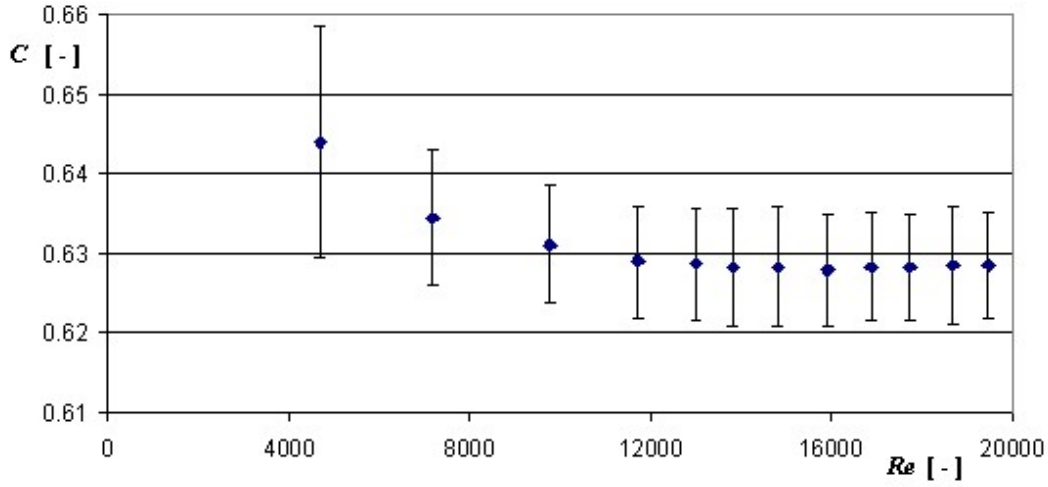

Figure 5. Value of discharge coefficient *C* depending on Reynolds number *Re*.

When analyzing the graph in Figure 5 we can assume that, for Reynolds numbers ranging $9800 \le Re \le 19500$, the values of discharge coefficient are close to a straight line and the values change only a little. This allows us to assume the constant average value of discharge coefficient at $C = 0.6286$ and bars representing errors of determining its absolute expanded uncertainty do not exceed ±0.0076.

4. Discussion

The article presented the results of experimental studies of a multi-opening orifice with substitute constriction factor $\beta = 0.5$, mounted in a DN50 hydraulic measuring channel. Based on the obtained averaged results from experiments, flow characteristics were determined and described with a simplified power equation with an exponent close to 0.5 with determination coefficient close to 1 which indicates a very good adjustment of the designated model (trend line) to the averaged results obtained from the experiment. Based on calculations from averaged measurement data, the value of discharge coefficient *C* was determined, along with estimating the uncertainty of determining it in a progressing turbulent flow for low Reynolds numbers (*Re* = 4700...19500) in laboratory conditions.

The presented study results for a multi-opening orifice (Fig. 1), with pressure measured in close proximity, indicating that for $Re \ge 9800$ numbers we observe the following:

- - there is constancy of discharge coefficient (its average value $C = 0.6286$) which is higher than the discharge coefficient for a centrical orifice by ca. 2.0% with the same constriction,
- - relative expanded uncertainty of determining discharge coefficient *U(C)/C* does not exceed 1.25% and is close in value to standardized orifices.

Further experimental studies are planned for a highly progressed turbulent flow (Re > 20000) including, among others, the influence of speed profile perturbation on the metrological properties of a multi-opening orifice.

Funding: This research received no external funding.

Conflicts of Interest: The author declares no conflict of interest.

References

1. Zhang, R.; Hang, Y. An Experimental Study of Pulsatile Flow In a Compliant Aortic Root Model dunder Varied Cardiac Outputs. *Fluids* **2018**. 3.71; doi:10.3390/fluids3040071.
2. Gondek, A. Przepływomierze spiętrzające przepływ (Flow meters that bank up the flow), *Politechnika Krakowska*. **2009**, (in Polish).
3. Kremlowski, P. P. Raschodimiery i scetciki kolicestva, vescestv. *Izd. Politechnika*. Saint Petersburg, **2002.**
4. Turkowski, M. Metrologia przepływów (Flow metrology) *Oficyna Wydawnicza Politechniki Warszawskiej*, Warszawa, **2018**, (in Polish).
5. EN ISO 5167-1: **2003** Measurement of fluid flow by means of pressure differential devices inserted in circular cross-section conduits running full - Part 1: General principles and requirements.
6. EN ISO 5167-2: **2003** Measurement of fluid flow by means of pressure differential devices inserted in circular cross-section conduits running full - Part 2: Orifice plates.
7. Golijanek-Jędrzejczyk, A.; Mrowiec, A.; Hanus, R.; Zych, M.; Świsulski, D. Uncertainty of mass flow measurement using centric and eccentric orifice for Reynolds number in the range 10,000 ≤ Re ≤ 20,000. *Measurement*. **2020,** Volume 160, August 2020, https.//doi.org/10.1016/j.measurement.2020.107851.
8. Tomaszewska-Wach, B.; Rząsa, M.R.; Majer, M. Measurement of two-phase gas-liquid flow using standard and slotted orifice. *IAPGOS*. **2019**, No. 4, pages 30-33, (in Polish), doi:10.35784/IAPGOS.47.
9. Bagade, V.S.; Suryawanshi, P.M.; Nalavade, S.M. A review of multi-hole orifice plate. *International Journal For Research in Applied Science and Engineering Technology*. **2019**, Volume 7, April, pages 3197-3208, https://doi.org/10.22214/ijraset.2019.4536.
10. Hao, C.Z.; Song, X.M.; Jia, Z.N. Influence of the hole chamfer on the characteristics of a multi-hole orifice flowmeter. *Fluid Dynamics and Materials Processing*. **2019,** Volume 15, No. 4, pages 391-401, DOI: 10.32604/fdmp.2019.07771.
11. Singh, V.K.; Tharakan, T.J. Numerical simulations for multi-hole orifice flow meter. *Flow Measurement and Instrumentation*. **2015,** Volume 45, October, pages 375-383, https://doi.org/10.1016/j.flowmeasinst.2015.08.004.
12. Guide to the Expression of Uncertainty in Measurement, Joint Committee for Guides in Metrology (JCGM) 100:**2008**.
13. Diaz, R. P.; Dalfre Filho, J. G.; de Lucca, Y. F. L. Water flow meter measurement uncertainties; Conference: *Water Resources Management 2013*. Volume 171. May, **2013**, DOI: 102495/WRM/130281.
14. Wiora, J.; Wiora, A. Measurement Uncertainty Calculations for pH Value Obtained by an Ion-Selective Electrode. *Sensors* **2018**. 18.1915; doi: 10.3390/s18061915.